New Aspects of Giant Exciton Faraday Rotation in $Cd_{1-x}Mn_xTe$ Semimagnetic Compound: Fundamentals and Applications

D. A. AKSIONOV, V. I. KONOV, P. I. NIKITIN, A. M. PROKHOROV, A. I. SAVCHUK,
A. V. SAVITSKI and K. S. ULYANITSKI

General Physics Institute, U.S.S.R. Academy of Sciences, 38 Vavilov Street, 117942 Moscow (U.S.S.R.)

Abstract

Wavelength, magnetic field, and temperature dependences of Faraday rotation (FR) in various compositions of the dilute magnetic semiconductors $Cd_{1-x}Mn_xTe$ and $Zn_{1-x}Mn_xTe$ have been experimentally investigated. Regularities of the Faraday effect dispersion connected with the change of rotation direction as a function of temperature and Mn concentration in the compound have been revealed. Deviation in FR saturation at helium temperatures and high magnetic fields is observed. According to the FR temperature dependence, the spontaneous Faraday effect is assumed to be a characteristic of the spin glass state of semimagnetic semiconductors. A rapid magnetic field sensor system as a possible application of this material has been proposed.

Introduction

One of the unique features of semimagnetic semiconductors is the unusually large Faraday effect that they exhibit. In $Cd_{1-x}Mn_xTe$ an unusually large spin splitting of exciton states and the accompanying giant strengthening of interband Faraday rotation has been observed for the first time [1, 2]. In these and the following papers attention was mainly drawn to any increase in the absolute FR and almost nothing was said about the direction of rotation. Only recently [3, 4] has the complicated behavior of the Faraday effect dispersion with the change of sign of rotation been pointed out. Theoretical explanations of the experiments on Faraday effect in semimagnetic $Cd_{1-x}Mn_xTe$ suffer from the drawback of using only a simple exciton mechanism.

Experimental Results

Solid solution $Cd_{1-x}Mn_xTe$ was grown using a modified Bridgman method. The experiments were performed on single crystal samples having concentration x up to 0.45 and a thickness of 0.1–10 mm.

First of all we noticed the spectrally dependent FR picture to be somewhat different from that reported in previous papers [1, 2]. Along with the strong absolute FR magnitude Θ increase compared to 'pure' CdTe at room temperature one can see (in Fig. 1) a change in rotation direction (from positive for CdTe to negative for $Cd_{1-x}Mn_xTe$). Moreover, for the sample with concentration $x = 0.007$ inversion of the sign of rotation occurs. The samples having $x > 0.05$ exhibit the negative FR right up to 0.6 eV photon energy. Of interest is the fact that in the vicinity of $E = 1.47$ eV ($\lambda = 0.85\,\mu m$) the magnitude of the Verdet constant remains invariable for concentrations $x = 0.05$–0.30 because of the equalizing influence of the forbidden band gap $E_g(x)$ and $\Theta(x)$.

In Fig. 2 the dependence of FR dispersion upon temperature is shown for the concentration $x = 0.007$ which is characterized by the inversion of the sign of rotation. One can see the inversion vanishing during both the temperature increase and decrease.
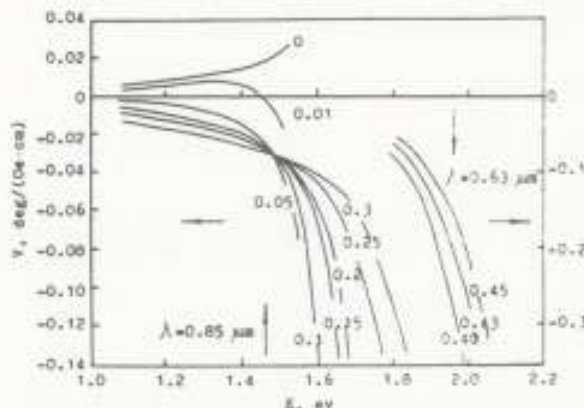

Fig. 1. Faraday effect spectral dependence of $Cd_{1-x}Mn_xTe$ for various compositions of Mn at $T = 300$ K.
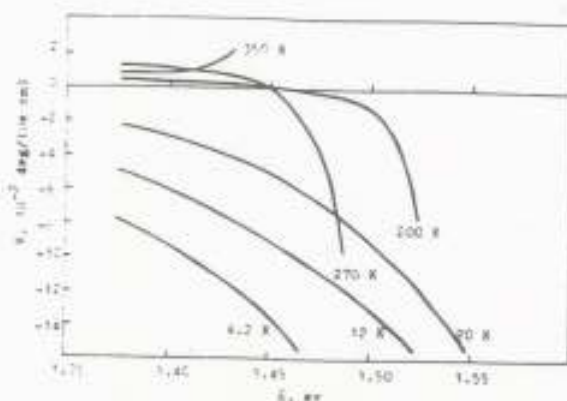
Fig. 2. Faraday rotation spectra of $Cd_{0.993}Mn_{0.007}Te$ for various temperatures.

Discussion

We consider the observed peculiarities in Faraday rotation spectral dependences for semimagnetic semiconductor $Cd_{1-x}Mn_xTe$ to be a result of the competition of different, opposite in sign contributions into the Faraday effect. In general, the $\Theta(E)$ dependence can be presented as a sum

$$\Theta(E) = \Theta_1(E) + \Theta_2(E) + \Theta_3(E) \qquad (1)$$

where $\Theta_1(E)$ is a characteristic of the interband Faraday rotation in the direct band semiconductors and can be written as the following equation

$$\Theta_1(E) = A\left[\frac{E_g^{3/2}(E_g-E)^{-1/2}}{E}\right.$$

$$\left. -\frac{E^{3/2}}{E}(E_g+E)^{-1/2} - 1\right] \quad (2)$$

For the contribution $\Theta_2(E)$, taking into account the electron-hole interactions, the following wavelength dependence is typical

$$\Theta_2(E) = B\left[\frac{E^2}{E_0^2 - E^2} + \frac{DE_0E^2}{(E_0^2 - E^2)^2}\right] \quad (3)$$

where E_0 is the energy location of exciton absorption zone maximum.

Writing the equations for A and B we must take into consideration the fact that the interband and exciton transitions can be characterized by the same spin splitting ΔE

$$A = A_1\Delta E; \quad B = B_1\Delta E; \qquad (4)$$

$$\Delta E = x\langle S_m\rangle N_0(J_h - J_e) + (g_h + g_e)\mu_b H \quad (5)$$

here $\langle S_m\rangle$ is the mean value of magneto-admixed subsystem magnetization, N_0 is the number of cation states per cm^3, $J_{e,h}$ are the exchange interaction integrals, $g_{e,h}$ are the effective g factors of electron and hole. Constants A_1, B_1 and D include zone and exciton characteristics of

crystals. Comparing eqns. (2)–(5) one can easily notice the signs of $\Theta_1(E)$ and $\Theta_2(E)$ to be determined by the negative ones of A and B because of $N_0(J_h - J_e) = -1.126$ eV for $Cd_{1-x}Mn_xTe$ crystals [5]. Admitting a satisfactory coincidence of the exciton contribution with the experimental results obtained earlier, it should be noted that in fact this occurs only at a small spectral region near the exciton transitions.

Nevertheless, only negative contributions are not sufficient for the explanation of the more complicated dependence $\Theta(E)$ with the sign of rotation inversion. Therefore let us examine the third positive contribution $\Theta_3(E)$, which can be expressed as

$$\Theta_3(E) = C\frac{E^2}{E_{ef}^2 - E^2}$$

where E_{ef} is the effective energy of transitions in the shortwave spectral region. The evaluation of E_{ef} was performed by the approximation of experimental data (Fig. 1) for $x = 0.007$ at 350 K in the wave gap $1-2$ μm (under such conditions $\Theta_1(E)$ and $\Theta_2(E)$ can be disregarded). The experimental points with sufficient precision lie on right line $V = \Theta/(Hd) \simeq (\lambda^2 - \lambda_{ef}^2)^{-1}$ and the obtained value of $\lambda_{ef} = (5100 \pm 200)$ Å, $E_{ef} = (2.43 \pm 0.1)$ eV agrees perfectly well with the intraband transition energy in Mn^{2+} ions.

In the magnetic field dependence of FR for the $Cd_{1-x}Mn_xTe$ compound (Fig. 3), besides the FR saturation at $H > 30$ kOe typical at helium temperatures one can observe its monotonous increase up to 250 kOe. We consider this to be a result of a step growth of magnetization $\langle S_m\rangle$ due to antiferromagnetic exchange interactions between the neighbouring Mn^{2+} ions. In the FR temperature dependence (Fig. 4) an abrupt decrease in the FR magnitude in the temperature
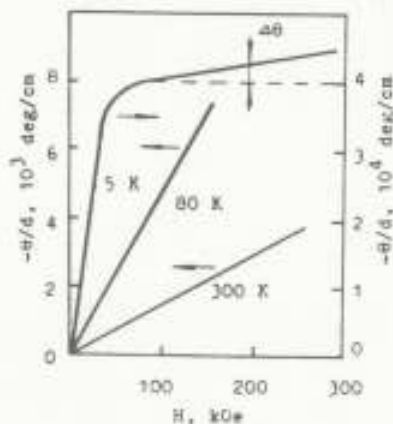

Fig. 3. Faraday effect magnetic field dependence of the $Cd_{0.93}Mn_{0.07}Te$ crystal at various temperatures.
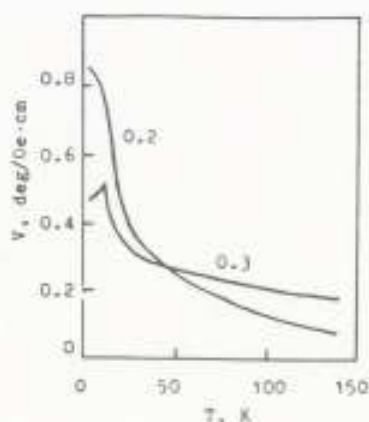
Fig. 4. Faraday effect temperature dependence at the absorption band region for two concentrations of Mn.

interval (4.2–50) K is observed, i.e. in accordance with the temperature dependence of magnetization $\langle S_m \rangle$. For the $\Theta(T)$ dependence of the $Cd_{0.9}Mn_{0.1}Te$ sample measured at low magnetic fields a certain maximum typical for the paramagnet to spin glass transition is seen. The evaluated transition temperature value $T_c = (11 \pm 0.5)$ K is in satisfactory agreement with the magnetic phase diagram of $Cd_{1-x}Mn_xTe$. Apparently differences in the rotation value for the spin glass state measured in low and strong magnetic fields (at $T < 11$ K) can be interpreted as a spontaneous Faraday effect.

Applications

One of the promising applications of $Cd_{1-x}Mn_xTe$ is the use of its strong FR for optical measurements of magnetic fields [6, 7]. In ref. 6 a crystal was used with $x = 0.45$ and $V = \Theta/(Hd) = 0.17$ deg/(Oe cm) for $\lambda = 0.63\,\mu m$. In our opinion, it is necessary to optimize the concentration of $Cd_{1-x}Mn_xTe$ for a more efficient use of it as a magnetooptical medium at a certain radiation wavelength. So we performed detailed measurements of V and of optical transmission near $\lambda_1 = 0.63\,\mu m$ for the He–Ne laser and near $\lambda_2 = 0.85\,\mu m$ for the injection laser. According to the measurements (Fig. 1), for λ_1 and for concentrations $x = 0.4, 0.43$ and 0.45, the Verdet constant was 0.32, 0.22 and 0.16 deg/(Oe cm) respectively. The concentration $x = 0.4$ with a maximal V is ultimate, since crystals with $x < 0.4$ are non-transparent for the emission with λ_1. It appears that for the He–Ne laser an optimal concentration is $x = 0.43$ for which V is larger than for $x = 0.45$ and the transmission coefficient

is at the level of $t \simeq 0.10$. Note that such an optimization also ensures a stable temperature regime for $Cd_{0.57}Mn_{0.43}Te$ samples, because for $x = 0.4$ slight variations in temperature can lead to significant changes in t and V parameters. To improve temperature stability of sensors the samples of $x > 0.45$ are preferable because for them the absorption edge is removed from the operation wavelength $\lambda_1 = 0.63\,\mu m$ and the temperature gradients of t and V are smaller.

Figure 5 illustrates the optical fiber magnetic field sensor design which has been produced using a He–Ne laser and the $Cd_{0.57}Mn_{0.43}Te$ crystal. The frequency dependence of the Faraday effect in such compounds is limited to frequencies of several GHz [8], therefore practically the sensor's operating band is determined in our case by a photodetector.

Our investigations also aimed at creating a susceptible sensor, so at a minimal level of the detected pulsed magnetic field $H_{mn} \simeq 1$ Oe, the operating band of the sensor at the level of -3 dB was as large as 140 MHz. This ensures a response time shorter than 3 ns. The sensor's susceptibility was 6 mV/Oe.

Concerning optimization of crystals for $\lambda_2 = 0.85\,\mu m$ it should be noted that it is unreasonable to use samples with small $x \simeq 0.05$ when λ_2 is near the absorption band edge. It has been noted above that near $E = 1.47$ eV V is independent of x $(0.05 \leqslant x \leqslant 0.45)$ and is 0.025 deg/(Oe cm) (Fig. 1). Therefore the use of high x crystals is also reasonable in this case, because at an increase in x the frequency band of the FR, its thermal stability and the transparency of the crystal also increase. Nevertheless, because of a smaller Verdet constant the susceptibility of such sensors is an order lower.

It appears that the picture with other solid solutions of the family $A^{II}_{1-x}Mn_xB^{VI}$ must be similar to that for $Zn_{1-x}Mn_xTe$ (large E_g values are typical for all of them). It has been established that for $Zn_{1-x}Mn_xTe$ the qualitative characteristics of concentration, spectral and magnetic field

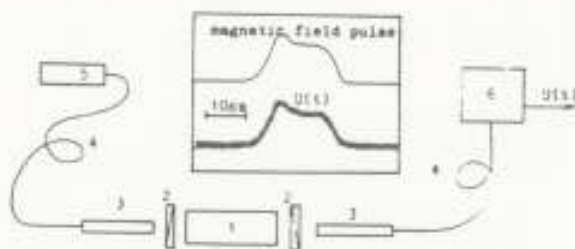Fig. 5. Optical fiber magnetic field sensor design: 1, $Cd_{1-x}Mn_xTe$ crystal; 2, cross polarizers; 3, gradient lens; 4, optical fibers; 5, laser source; 6, photodetector.
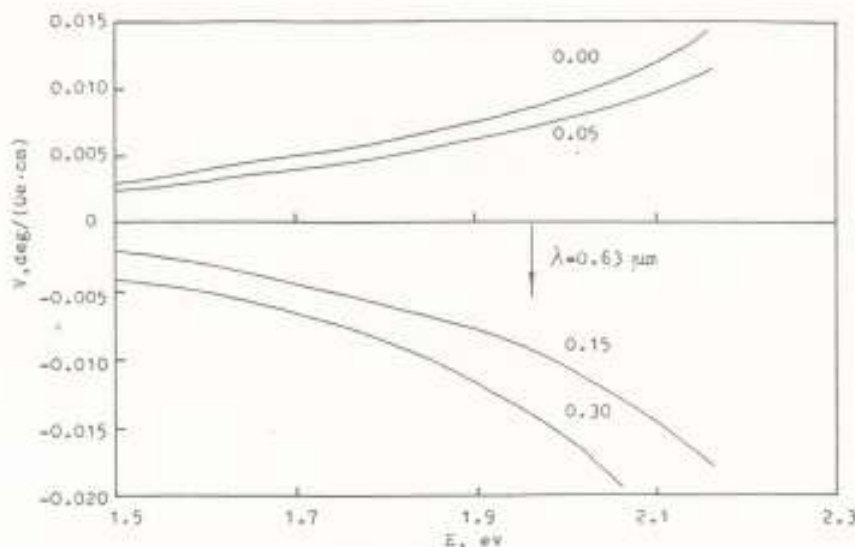
Fig. 6. Faraday effect spectral dependence of semimagnetic $Zn_{1-x}Mn_xTe$ for various compositions of Mn at room temperature.

dependences of FR are similar to those observed in $Cd_{1-x}Mn_xTe$. There is no doubt about the commonness of the physical mechanisms reported above that underlie such anomalies for various semimagnetic semiconductors. However, the data for $Zn_{1-x}Mn_xTe$ (Fig. 6) contain a quantitative difference in the absolute magnitude of FR. An essential decrease in V for this semiconductor results from two factors. Firstly, ZnTe, as compared to CdTe, has a smaller oscillator force of the exciton transition. Secondly, $\Theta_3(E)$ influences a total FR more strongly in $Zn_{1-x}Mn_xTe$ as in a more broad-band semiconductor and compensates the strong negative rotation. Furthermore, of particular interest are crystals for which $N_0(J_h - J_e) > 0$. Then the signs of all of the contributions Θ will be greater than zero.

Another way of enlarging the class of semimagnetic semiconductors to be more suitable for practical applications at room temperatures is to master four-component $A^{II}B^{VI}$ solid solutions. For example, in $Cd_xMn_yHg_{1-x-y}Te$ by varying the x and y concentrations it is possible to optimize a magnetooptical material for semiconductor lasers with $\lambda = 0.85$ or 1.a3 μm.

References

1 A. V. Komarov, S. M. Ryabchenko, O. V. Terletski, I. Izheru and D. Ivanchuk, Magneto-optical investigations and double optico-magnetic resonance of the exciton band in $CdTe:Mn^{2+}$, Zh. Eksp. Teor Fiz., 73 (1977) 608–618 (in Russian).

2 J. A. Gaj, R. R. Galazka and M. Nawrocki, Giant exciton Faraday rotation in $Cd_{1-x}Mn_xTe$ mixed crystals, Solid State Commun., 25 (1978) 193–197.

3 D. U. Bartholomev, J. K. Furdyna and A. K. Ramdas, Interband Faraday rotation in diluted magnetic semiconductors: $Zn_{1-x}Mn_xTe$ and $Cd_{1-x}Mn_xTe$, Phys. Rev. B, 34 (1986) 6943–6957.

4 A. I. Savchuk, B. E. Derkach, P. P. Vatamanyuk, A. V. Savitski and K. S. Ulyanitski, Characteristic properties of Faraday-rotation dispersion in semimagnetic semiconductors, Fiz. Tekh. Poluprovod., 22 (1988) 512–519 (in Russian).

5 R. L. Aggarwal, S. N. Jasperson, P. Becla and R. R. Galazka, Optical determination of the antiferromagnetic exchange constants between nearest-neighbor Mn^{2+} ions in $Cd_{0.95}Mn_{0.05}Te$, Phys. Rev. B, 32 (1985) 51–81.

6 M. A. Butler and S. J. Martin, Optical fiber magnetic field sensor with nanosecond response time, Proc. Transducers '85, Philadelphia, PA, U.S.A., June 11–14, 1985 pp. 101–105.

7 D. A. Aksionov, V. I. Konov, P. I. Nikitin, A. M. Prokhorov, A. I. Savchuk, A. V. Savitski and K.S. Ulyanitski, Faraday effect in the dilute magnetic semiconductor $Cd_{1-x}Mn_xTe$, Proc. XVIII Conf. Physics of Magnetic Phenomena, Kalinin, 1, 1988, pp. 147–148 (in Russian).

8 M. A. Butler, S. J. Martin and R. J. Baughman, Frequency-dependent Faraday rotation in CdMnTe, Appl. Phys. Lett., 49 (1986) 1053–1056.